

Article

Particle Swarm Optimization Method for Stand-Alone Photovoltaic System Reliability and Cost Evaluation Based on Monte Carlo Simulation

Eduardo Quiles-Cucarella ^{1,*} , Adrián Marquina-Tajuelo ¹, Carlos Roldán-Blay ²  and Carlos Roldán-Porta ² 

¹ Instituto de Automática e Informática Industrial, Universitat Politècnica de València, Camino de Vera, s/n, 46022 Valencia, Spain; admarta1@etsii.upv.es

² Institute for Energy Engineering, Universitat Politècnica de València, Camino de Vera, s/n, Building 8E, 46022 Valencia, Spain; carrolbl@die.upv.es (C.R.-B.); croidan@die.upv.es (C.R.-P.)

* Correspondence: equiles@isa.upv.es; Tel.: +34-963877007

Abstract: In rural regions with limited access to the power grid, self-reliance for electricity generation is paramount. This study focuses on enhancing the design of stand-alone photovoltaic installations (SAPV) to replace conventional fuel generators thanks to the decreasing costs of PV modules and batteries. This study presents a particle swarm optimization (PSO) method for the reliable and cost-effective sizing of SAPV systems. The proposed method considers the variability of PV generation and domestic demand and optimizes the system design to minimize the total cost of ownership while ensuring a high level of reliability. The results show that for the PSO method with 500 iterations, the error is around 2%, and the simulation time is approximately 2.25 s. Moreover, the PSO method allows a much lower number of iterations to be used in the Monte Carlo simulation, with a total of 100 iterations used to obtain the averaged results. The optimization results, encompassing installed power, battery capacity, reliability, and annual costs, reveal the effectiveness of our approach. Notably, our discretized PSO algorithm converges, yielding specific parameters like 9900 W of installed power and a battery configuration of five 3550 Wh units for the case study under consideration. In summary, our work presents an efficient SAPV system design methodology supported by concrete numerical outcomes, considering supply reliability and installation and operational costs.

Keywords: renewable energy; photovoltaic generation; reliability; Monte Carlo simulation; PSO



Citation: Quiles-Cucarella, E.; Marquina-Tajuelo, A.; Roldán-Blay, C.; Roldán-Porta, C. Particle Swarm Optimization Method for Stand-Alone Photovoltaic System Reliability and Cost Evaluation Based on Monte Carlo Simulation. *Appl. Sci.* **2023**, *13*, 11623. <https://doi.org/10.3390/app132111623>

Academic Editors: S. M. Muyeen, Mohamed Benbouzid and Muhammad Fahad Zia

Received: 14 September 2023

Revised: 10 October 2023

Accepted: 11 October 2023

Published: 24 October 2023



Copyright: © 2023 by the authors. Licensee MDPI, Basel, Switzerland. This article is an open access article distributed under the terms and conditions of the Creative Commons Attribution (CC BY) license (<https://creativecommons.org/licenses/by/4.0/>).

1. Introduction

Stand-alone photovoltaic systems (SAPV) are becoming more popular in rural areas, where there is typically no access to the electricity distribution network (DN) under profitable economic conditions [1–7]. An SAPV system cannot be designed until the rated power of the PV panels and the battery storage capacity are known. PV generation is irradiation-dependent, which causes uncertainty in its energy output [8,9]. Both in the short term (hour-to-hour variations) and the long term (seasonal variations), this irradiation level differs significantly between sunny and cloudy days [10,11]. Even on a typical day with a clear sky, passing clouds can cause fluctuations in PV power. A trustworthy forecast of a device's reliability is necessary to improve SAPV's sustainability. It is practical to carry out a thorough analysis of the solar radiation characteristics close to the SAPV installation. PV generation uncertainty must be modeled to project average performance in the future. Solar radiation time-series measurements from nearby weather stations are required [12–14] to calculate expected generation.

Energy use in residential households and PV generation barely overlap. PV generation is at its peak at noon, while residential customers typically experience their peak period in the evening. The battery system enables the daytime PV energy surplus to be stored. The additional PV energy will be utilized to recharge the battery as long as it has not reached

its maximum state of charge (SOC). To increase self-sufficiency, demand-side management can be used to shift the consumption of deferrable loads to times when PV systems have surpluses [15,16].

To design a realistic SAPV system, an accurate load demand model is required. This is particularly difficult for residential customers who frequently have a fluctuating load profile. Residential load is temporally variable and depends on the time of day, the day of the week, and the season of the year. To simulate the energy flows between the PV unit, battery, and load, time series data of PV generation and load demand with a high temporal resolution are required.

Numerous studies have been carried out to determine the viability of SAPV systems [17]. There are studies [18–21] that analyze residential PV plants connected to the DN. Through this connection, they can sell energy surpluses to the utility and import energy from the DN as needed. Various studies [22,23] consider SAPV systems that are autonomous and unconnected to the DN. This is frequently the only choice in many rural areas. Different methods for designing such SAPV systems have been proposed. Finding the most dependable and cost-effective PV unit and battery configuration for energy generation and storage is the main objective. Some authors offer solutions on the basis of equations for the energy balance [24]. Some of them use statistical techniques to account for variations in solar radiation [12]. A list of SAPV system-sizing methods can be found in [1,25].

For the SAPV design to be successful while taking into account the reliability of the associated systems, a realistic model of the energy resource, energy demand, and component failures is necessary. In many studies, average solar irradiance levels over a wide area are frequently considered. These data come from the meteorological service's databases and represent monthly averages [26,27]. This study measures local hourly irradiance levels and takes them into consideration during the design stage.

As mentioned earlier, residential demand varies significantly depending on the user and the day. The oversimplified method of using an average daily peak demand is obviously a significant understatement of the demand fluctuation [1]. In this work, actual hourly demand data from typical customers are considered.

The temporal resolution of PV generation and load demand also affects how applicable simulation results are. The power balance between PV generation and energy consumption must be reflected at least hourly [28–30]. Lower temporal resolutions (10 min sampling data) have been proposed by certain authors [1] to evaluate energy flows between PV units, batteries, and loads.

SAPV systems are a commercially viable and cost-effective solution for residential users without access to the DN, according to many research works [31]. The initial expenses of PV panels, batteries, and installation have an amortization period that is less than the PV plant's useful life, according to [18,32]. Because of this, for many residential customers, the reliability of the electrical supply—rather than the expense of the investment—is the most important aspect to consider when planning the installation of an SAPV system. As long as there is a high level of supply reliability guaranteed, many private home investors are willing to pay the investment costs of the PV generation system [33]. Because of this, an optimal design process for the SAPV system is necessary, one that takes into account all of the system's uncertainties.

During SAPV design, unanticipated system faults must be considered assuming no component faults can result in an overly optimistic performance prediction and the consequent undersizing of PV modules and batteries [34].

Monte Carlo simulation (MCS) techniques can be executed sequentially or non-sequentially [35]. By sequentially sampling the states of the system's component parts, the sequential MCS simulates the chronology of the stochastic process of system operation. The earlier states, such as the battery's SOC status, determine the current state of a renewable energy system with energy storage. Typically, there is no connection between residential demand and PV generation. The complexity of this reliability analysis is better handled by

a sequential MCS. Other methodologies, such as reliability evaluation based on analytical models or Markov models, cannot be used to realistically evaluate SAPV systems [36].

Sequential Monte Carlo simulation is used in this study to assess component faults. The paper's goal is to size the SAPV system economically optimally while imposing some restrictions on the system's intended reliability. This study is distinct from previous ones in that it considers actual data from time series on PV generation and load demand in addition to the simultaneous evaluation of uncertainties related to faults in system components. The aim of the design of an SAPV generation system is to guarantee the desired level of reliability in the continuity of the supply. The problem is formulated as a single-objective cost optimization problem, as the reliability of the SAPV system is set as a minimum requirement. To calculate the optimal size of the installation that minimizes investment and operation costs for a minimum established reliability requirement, the application of an evolutionary algorithm (EA) has been considered. An evolutionary algorithm is an optimization method that imitates behaviors of nature to obtain an approximate solution of non-linear complex optimization problems, with a large number of variables or very complex to solve using traditional mathematical algorithms [37]. The first to be described was the genetic algorithm (GA), although there is currently a wide variety of alternatives, such as the particle swarm optimization (PSO) algorithm based on bird behavior, the ACO algorithm (ant colony optimization) based on the behavior of ant colonies, or evolutions and variants of these such as the memetic algorithm (MA). Different studies have been published comparing the EA, both qualitatively [38], and comparing the performance in solving optimization problems of different kinds. While, qualitatively, advantages and disadvantages are observed in each one of them, quantitatively, in the studies where the performance of each one of them has been compared, the PSO algorithm on average reaches the solution more quickly and effectively [37,39]. This fact, added to its simplicity, positions it as the one indicated to implement in this work. The PSO algorithm was devised by Kennedy and Eberhart in 1995 to describe the behavior of fish and birds. It has been used to describe the behavior of complex systems to reach an optimal solution [40].

The objective of this work is the application of an optimization method based on PSO to minimize the costs associated with the investment and operation of an SAPV system for a guaranteed level of reliability. The proposed method implements the following improvements over previous contributions:

- Simultaneous consideration of uncertainty in PV generation and domestic demand and modeling the occurrence of random faults affecting the system.
- Calculation of the total cost of the installation based on the direct investment costs, as well as the costs of energy to be provided in hours when an auxiliary fuel generation system must operate.
- Introduction of the reliability evaluation method based on Monte Carlo sequential simulation in a cost optimization process using PSO.
- The use of real-world demand and irradiance data from PVGIS [41] and datasheets from commercial photovoltaic modules.

What sets this study apart is the utilization of real-world data spanning an entire year, as opposed to relying solely on typical values. This real data integration adds a crucial layer of authenticity to this research, ensuring that the findings are rooted in practical, real-world scenarios.

Moreover, this research goes beyond conventional analyses by offering a comprehensive discussion section. Thorough comparisons are conducted, enabling a deeper understanding of the design, costs, and reliability aspects of SAPV systems. This holistic approach allows us to take the analysis one step further and provide optimal results.

Section 2 of this manuscript presents the energy balance in an SAPV system, a reliability evaluation method performing sequential Monte Carlo simulation, and the optimization method to minimize SAPV investment and operation costs subjected to the desired reliability level of the electric supply. In Section 3, the results of the proposed method are validated against an iterative algorithm, and a particular case study is evaluated. In Section 4, a

discussion of the results takes place, as well as some additional considerations and findings obtained from the sensitivity analysis performed. Finally, in Section 5, some conclusions about the advantages of the proposed method for SAPV design are drawn.

2. Materials and Methods

In this section, a detailed, step-by-step description of the research methods employed in this study is provided. First, the SAPV system and its components are introduced. Secondly, an explanation of how the energy demand was modeled and the methods for evaluating reliability and optimizing costs are presented.

2.1. Stand-Alone Photovoltaic Energy System

PV renewable generation has been installed in many residential homes to meet their own energy needs. Batteries are used in conjunction with this generation to store energy during times of surplus and to provide energy during periods of insufficient PV output. A typical installation of photovoltaic panels and batteries to power an off-grid residential load is shown in Figure 1. The battery is equipped with a regulator or battery controller (BC) to adjust SOC and maximum current during charging and discharging. Power flows between the battery and the PV panel array are decided by the BC.

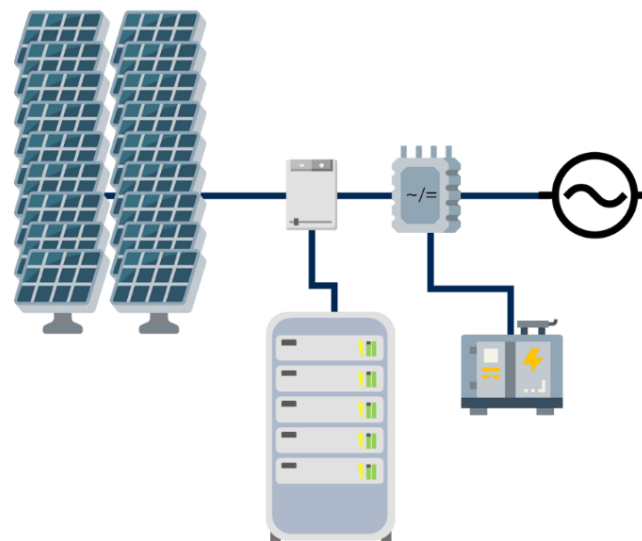


Figure 1. Stand-alone photovoltaic (SAPV) system scheme.

A conventional auxiliary generator is additionally considered to provide energy in the hours in which the main system (PV + batteries) does not meet the supply—in this case, a fuel generator set.

In this study, time series data with a temporal resolution of one hour were registered to model a typical household's energy demand. Figure 2 displays typical seasonal values for a residential customer's daily demand.

An approximate instantaneous generation power is estimated from solar irradiance and temperature data collected in the PVGIS tool [41]. In this database, data from different years are registered, in addition to having data from typical meteorological years (TMY). In a TMY, the annual data are formed from the data set of previous years, taking the values that are considered average or typical for a location.

The effects of the irradiance variation in the nominal generation of the module and the effects of the temperature in the installation are considered according to Equations (1) and (2).

$$T_{\text{cell}} = T_{\text{amb},i} + G_i * \frac{\text{NOCT} - 20}{800} \quad (1)$$

$$P_{g_i} = \frac{G_i}{G_{STC}} * P_N * (1 + \gamma * (T_{cell} - 25)) \tag{2}$$

where:

T_{cell} : Temperature of the photovoltaic cell.

T_{amb} : Ambient temperature at the location.

G_i : Instantaneous global irradiance value on the module.

NOCT: Nominal operating cell temperature ($45 \pm 2 \text{ }^\circ\text{C}$).

G_{STC} : Irradiance under standard test conditions (1000 W/m^2).

γ : Coefficient of percentage variation in power with temperature.

If the term P_N is eliminated from this equation, it is normalized, so that it can be used in an iterative method for designing the installation, multiplying by the installed power in each case.

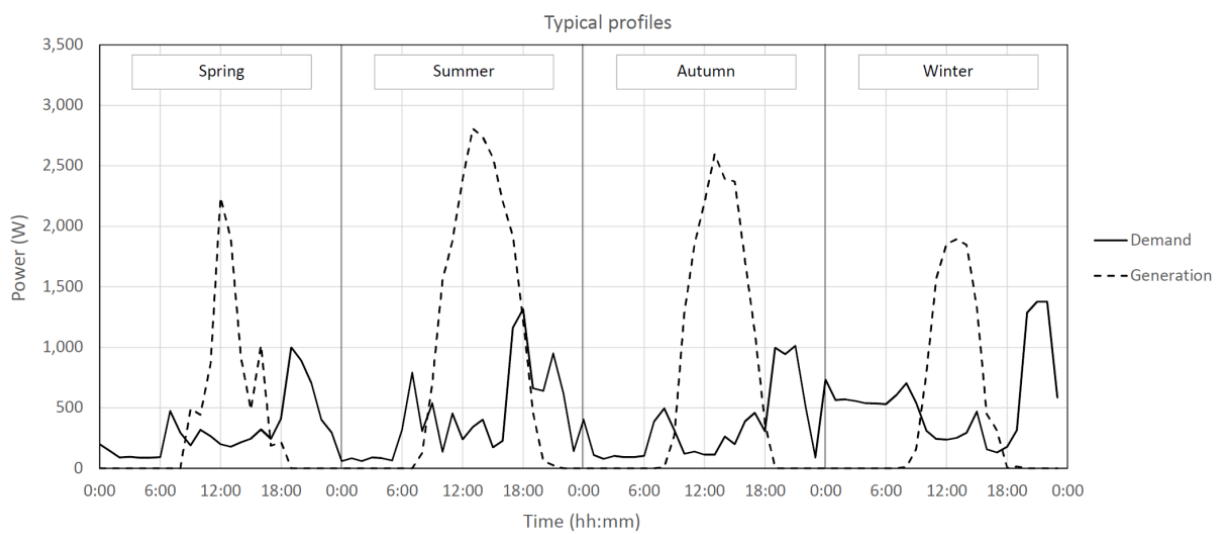


Figure 2. Seasonal residential customer daily load profile and hourly generation curve.

On the other hand, in order to have an adequate demand model, consumption data for a household over a year have been obtained, which will be used as a profile to generate the system load time series.

The energy balance of the system is evaluated as the balance at the terminals of the battery, i.e., the energy that contributes to charging or discharging it (Equations (3) and (4)).

$$E_{b,i} = (E_{g,i} - E_{d,i}) * \eta_c, \quad E_{g,i} > E_{d,i} \tag{3}$$

$$E_{b,i} = \frac{(E_{g,i} - E_{d,i})}{\eta_d}, \quad E_{g,i} < E_{d,i} \tag{4}$$

where:

$E_{b,i}$: energy that the battery can return in a daily discharge cycle in period i .

$E_{g,i}$: average daily energy generation in period i .

$E_{d,i}$: average daily energy demand in period i .

η_c : battery charging efficiency.

η_d : battery discharge efficiency.

Once the energy that charges/discharges the battery at each instant has been obtained, the equation that determines the state of charge can be evaluated (Equations (5) and (6)).

$$Q_{b,i} = Q_{b,i-1} + E_{b,i} \quad \text{if } Q_{b,i-1} > SOC_{min} \tag{5}$$

$$\text{SOC} = \frac{Q_{b,i}}{Q_{b,\max}} \quad (6)$$

where:

$Q_{b,i}$: battery capacity at period i .

$Q_{b,i-1}$: battery capacity at period $i - 1$.

$Q_{b,\max}$: maximum battery capacity.

SOC_{\min} : Minimum state of charge for the battery.

The state of charge of the battery has limits. A minimum charge of 20% is established to prolong battery life. For the periods in which the battery is at 20%, the SAPV system will be considered to have not delivered the necessary energy supply, and the undelivered energy demand will be counted as energy not supplied (ENS). On the other hand, if the battery reaches its maximum charge, the excess generated energy that cannot be consumed or stored will be counted as energy not used (ENU).

ENS represents the total energy in a year that the SAPV installation has not covered the requested electricity demand. This energy will be considered for the purpose of evaluating the costs that come from the operation of the backup fuel generator set.

2.2. Reliability Evaluation Method

Two questions must be answered in order to assess the SAPV system's reliability. If the combined instantaneous power from the PV arrays and the energy stored in the batteries is insufficient to meet demand, there will be a supply interruption. The occurrence of unanticipated system faults is the second reason for a supply interruption.

A PV plant's reliability model is a complicated subject [42–44]. An aggregated PV plant reliability model (including PV panels and BC) with a failure rate λ_c is employed to achieve the goals of this study. It is assumed that the PV plant's reliability model has two states, with total power output in the up state and zero power output in the down state. Batteries' faults are not taken into account because it is assumed that they will be maintained and replaced before reaching the end of their useful life (so it is assumed that $\lambda_b = 0$).

The PV plant's time to failure (TTF) and mean time to repair (TTR) are both modeled using exponential and Rayleigh distributions, respectively [45]. Utilizing the inverse transform method, TTF and TTR are generated at random [46].

When a PV panel array or BC fails, the PV generation curve becomes zero when the sequence of failures is combined with it. The generating capacity sequence (GCS) is acquired in this manner. Then, the GCS and the demand sequence are combined to determine the battery's SOC.

SOC(t) is obtained from Equation (7) by taking into account the instantaneous power demand $P_d(t)$ and GCS(t):

$$\text{SOC}(t) = \text{SOC}(t - 1) + \alpha(\text{GCS}(t) - P_d(t)) \cdot \Delta t, \quad (7)$$

where $\alpha = \eta_c$ if $\text{GCS}(t) - P_d(t) > 0$ and $\alpha = 1/\eta_d$ if $\text{GCS}(t) - P_d(t) < 0$.

An interruption of supply due to generation inadequacy occurs when:

$$\text{SOC}(t) \leq \text{SOC}_{\min} \text{ and } \text{GCS}(t) < P_d(t). \quad (8)$$

The energy supplied by the battery is assessed using Equations (7) and (8) during PV failure periods to reduce the failure time completely or partially until the battery is discharged to SOC_{\min} . The frequency of interruptions (FOI in number of interruptions/yr) and the loss of energy expectation (LOEE in Wh/yr) are evaluated according to the reliability analysis method.

There is a capacity for producing energy that cannot be used (ENU) if $\text{SOC}(t) = \text{SOC}_{\max}$ and $\text{GCS}(t) > P_d(t)$.

The variables $P_s(t)$ and $P_d(t)$ must be discretized in order to use the analysis method numerically. The energy generated by the PV array is calculated for each hour h of the year,

and its value is assigned to the discrete variable $P_s(h)$. Its value can be expressed in both kW and kWh, which are equivalent units of measurement, because it relates to average hourly power. If the discrete values of $P_s(h)$ are used to calculate the $GCS(t)$, then $GCS(t)$ is automatically discretized as $GCS(h)$. An analogous discrete variable, $P_d(h)$, is used to represent the energy required for each hour.

The system's hourly behavior for a sequence of n years is simulated using a sequential Monte Carlo simulation (MCS). To create chronological generation and demand random sequences, the randomized irradiance level for each hour of the day for each month of the year is taken into account along with the hourly demand.

The reliability evaluation method is carried out as explained in [47]:

- BEGIN: Set up the counter with $n = 1$. Obtain the initial system settings.
- FOR $n = 1$ to n DO:
 - Initialize the following counters: $h = 1$ (number of simulated hours of the year); $i = 0$ (counter of interruptions); $H = 0$ (hours of interruption); $LOEE = 0$; $ENU = 0$, $SOC = 80\%$ (battery state of charge).
 - To create the annual failure sequence, simulate TTF and TTR in turn.
 - Using data from the historical record generate randomized hourly PV generation time series data $P_s(h)$.
 - Using data from the historical record generate the hourly chronological curve of annual demand $P_d(h)$.
 - Combine $P_s(h)$ and the annual failure sequence to get the generating capacity sequence $GCS(h)$ for the simulated year.
 - FOR $h = 1$ to 8760 DO:
 - Using $GCS(h)$ and $P_d(h)$, solve Equation (7) to get $SOC(h)$.
 - Update the number of interruptions i and evaluate the duration in hours of each interruption H_i .
 - If $SOC = SOC_{min}$ and $GCS(h) < P_d(h)$, update $LOEE$: $LOEE = LOEE + P_d(h) - GCS(h)$.
 - If $SOC = SOC_{max}$ and $GCS(h) > P_d(h)$, update ENU : $ENU = ENU + GCS(h) - P_d(h)$.
 - Determine FOI index: $FOI = i$.
 - Assess the loss of load expectation (LOLE) index: $LOLE = \sum H_i$ (h/yr).
 - Assess the loss of load probability (LOLP) index: $LOLP = 100 \cdot LOLE / 8760$.
 - Evaluate average values of the indices for the n simulated years (Consider a possible convergence criterion).
- Evaluate reliability indices frequency histograms per year.

To establish a number of iterations to make the probabilistic calculation with an acceptable error, a study of the standard deviation of the averaged LOLP index is carried out as a function of the number of repetitions, taking into account the time used by the simulation (Figure 3).

Above 500 iterations, the error is around 2%, with a simulation time of approximately 2.25 s. From this point on, the error reduction function becomes horizontally asymptotic, while the execution time increases proportionally to the iterations. To reduce the error to 1%, the execution time is multiplied five times. Carrying out tests of the code, it has been observed that with 500 repetitions, errors occur in the convergence of the program. For that reason, the number of iterations has been increased to 1000. Figures 4 and 5 show the reliability indices average as a function of the number of iterations.

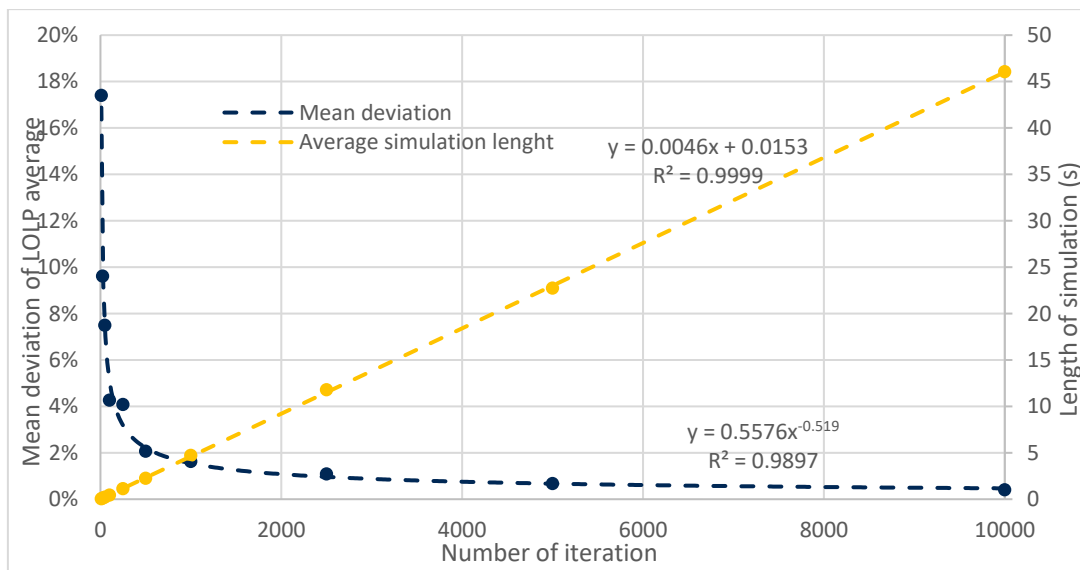


Figure 3. Error of the result and simulation time versus number of iterations.

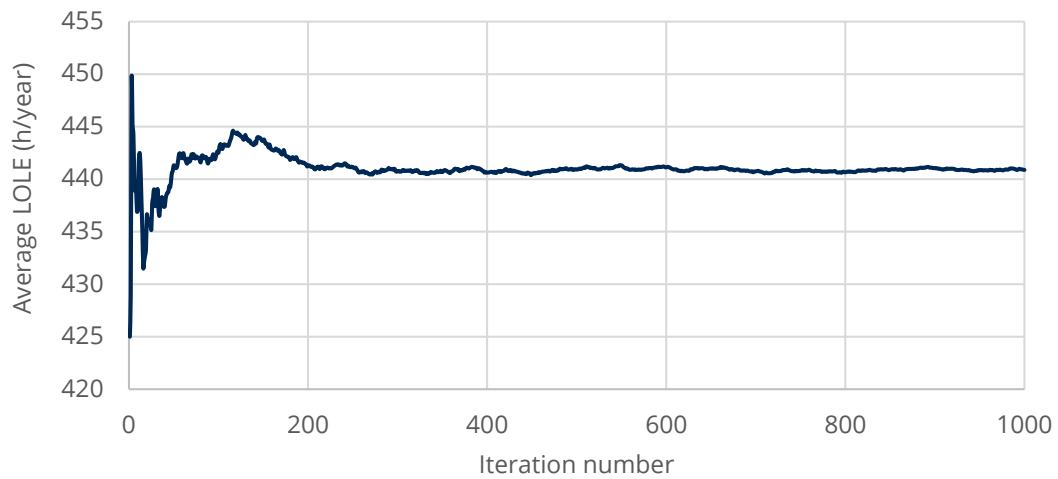


Figure 4. Value of the LOLE index as a function of the number of iterations.

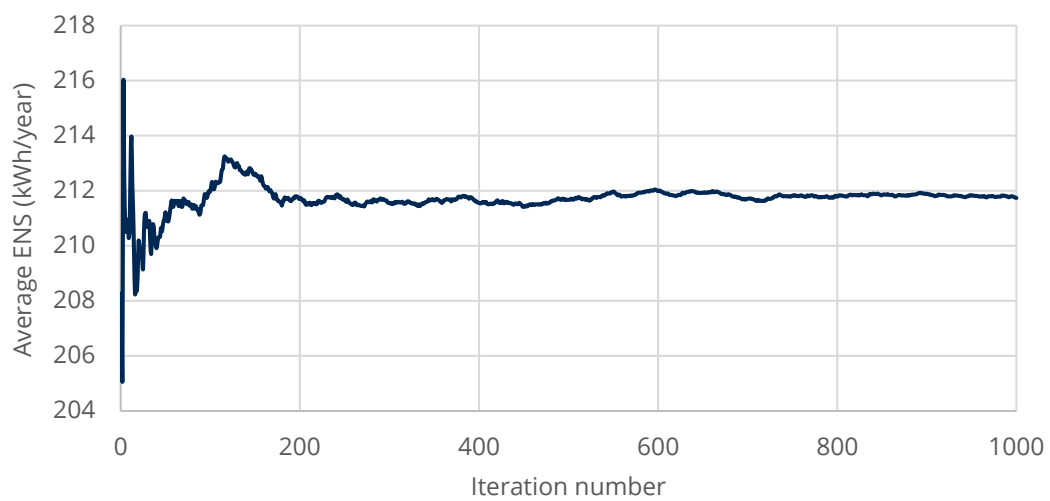


Figure 5. Value of the ENS index as a function of the number of iterations.

2.3. Optimization Problem

The primary objective of this section is to minimize the total cost associated with the SAPV. The objective function, as described in Equation (9), incorporates various cost components:

$$\text{Annual}_{\text{cost}} = \text{PV}_{\text{cost}} + \text{Battery}_{\text{cost}} + \text{Generator}_{\text{cost}} \tag{9}$$

Each of these components must be optimized to achieve the minimum annual cost. This optimization involves selecting the most efficient combination of installed PV panel power and battery capacity. The specific definitions for these terms are provided as follows:

$$\text{PV}_{\text{cost}} = \frac{P_{g,\text{installed}} * \text{costWh}_{\text{installed}}}{\text{useful_Life}_{\text{panels}}} \tag{10}$$

$$\text{Battery}_{\text{cost}} = \frac{Q_{b,\text{max}} * \text{costWh}_{\text{installed}}}{\text{useful_Life}_{\text{battery}}} * \frac{\text{useful_Life}_{\text{panels}}}{\text{useful_Life}_{\text{battery}}} \tag{11}$$

$$\text{Generator}_{\text{cost}} = \text{Fuel}_{\text{cost}} \left(\frac{\text{euros}}{\text{T}} \right) * \text{ENS}(\text{kWh}) * \text{Generator_consumption} \left(\frac{1}{\text{kWh}} \right) \tag{12}$$

In order to solve this optimization problem, certain constraints must be satisfied. These constraints ensure that the equipment sizes are physically feasible and prevent the system cost from escalating to excessively high values. Specifically, the constraints are shown in Equations (13)–(16).

Equipment size constraints:

$$P_{g,\text{installed}} \geq 0 \tag{13}$$

$$Q_{b,\text{max}} \geq 0 \tag{14}$$

Size limit constraints:

$$P_{g,\text{installed}} \leq 20,000 \tag{15}$$

$$Q_{b,\text{max}} \leq 35,000 \tag{16}$$

The final mathematical formulation of the optimization problem can be summarized as follows:

$$\begin{aligned} & \min \quad \text{Annual}_{\text{cost}} \\ & \text{subject to} \quad \begin{cases} P_{g,\text{installed}} \geq 0 \\ Q_{b,\text{max}} \geq 0 \\ P_{g,\text{installed}} \leq 20,000 \\ Q_{b,\text{max}} \leq 35,000 \end{cases} \end{aligned} \tag{17}$$

This formulation defines the objective function and constraints required to optimize the SAPV system’s design while minimizing annual costs, ensuring equipment sizes are positive, and preventing sizes from exceeding predefined limits.

The optimization problem addressed is formulated as a mono-objective optimization problem. It is aimed to minimize a single cost function, which represents the overall cost associated with the design and operation of the stand-alone photovoltaic (SAPV) system. However, the implications of the design results on reliability are also studied, taking advantage of Monte Carlo simulations.

2.4. Cost Optimization Algorithm

To solve the optimization problem indicated in Equation (17), the following procedure is used. Due to the fact that it is an SAPV system, the useful usable energy will be taken into account (usable energy = total generated energy – ENU).

To calculate the optimal size of the SAPV installation that minimizes investment and operation costs for a minimum established reliability objective, an evolutionary optimization algorithm based on PSO has been implemented. This algorithm starts from a swarm or society of particles initially uniformly distributed in the space of possible solutions for battery storage capacity and installed PV power, as seen in Figure 6. The particles meet the following requirements:

- The dimensions of the space are known, as well as the value of the objective function for each particle, although its maximum/minimum is not known.
- Particles can move freely through space.
- Particles have memory, remembering the position of their own optimum.
- There is communication between particles, knowing all the positions and values of the global optimum.

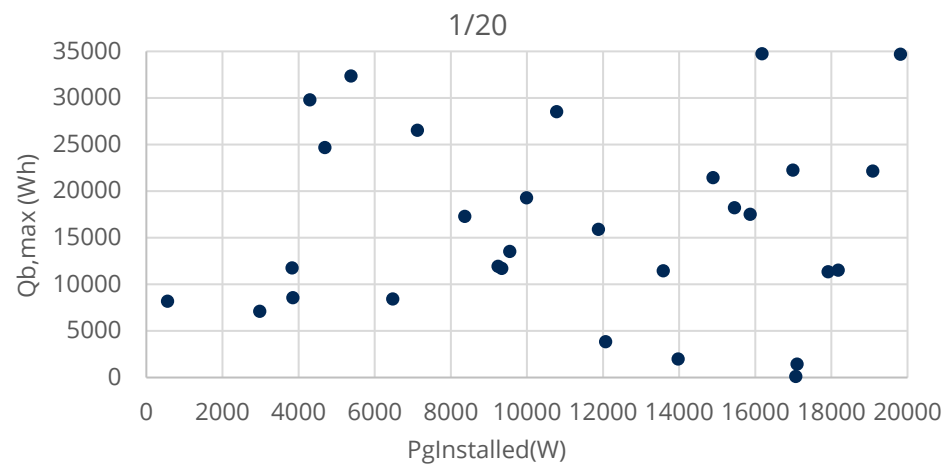


Figure 6. Initial position of the particles in the state space of the PSO algorithm.

For this initial distribution, the value of the objective function of each particle is calculated. This value becomes its own optimum and the global optimum is established among all of them. In the successive iterations of the algorithm, the particles will begin to move according to Equation (11).

$$\vec{x}_i(t + 1) = \vec{x}_i(t) + \vec{v}_i(t + 1) \tag{18}$$

where:

- $x_i(t)$ is the position of particle i at time t .
- $v_i(t + 1)$ is the speed of particle i at time $t + 1$.

Both position and velocity are treated as dimensionless parameters, since to be dimensionally correct, the velocity at one instant should be multiplied by the time at the next instant. The time between instants is considered to be one iteration, leaving the parameter multiplied by one, so it is a displacement to the next point.

Thus, the behavior of the particle is defined with a simple kinematics equation where the new position is the current position plus a velocity vector (Equation (12)).

$$\vec{v}_i(t + 1) = w_{damp}^t * w * \vec{v}_i(t) + r_1 * c_1 (\vec{p}_i(t) - \vec{x}_i(t)) + r_2 * c_2 (\vec{g}_i(t) - \vec{x}_i(t)) \tag{19}$$

where:

- w_{damp}^t is the damping coefficient raised to iteration t .
- w is the coefficient of inertia of the particle.
- r_1 and r_2 are two normalized positive random vectors.
- c_1 and c_2 are the cognitive and social coefficients, respectively, of the particle.
- p_i is the position of the particular optimum of the particle.

g_i is the position of the global optimum of the swarm.

Three terms can be distinguished in the equation. The first of them is the inertial term ($w_{\text{damp}}^t * w * \vec{v}_i(t)$), which considers the movement that the particle previously had and contains a damping coefficient that decreases it with the passing of the iterations in order to prevent the particle from oscillating as it converges to the final solution. The second term ($\vec{r}_1 * c_1 (\vec{p}_i(t) - \vec{x}_i(t))$) is cognitive. It considers the distance from the particle's position to its own historical optimum, updating itself if it finds a new one. Finally, the third term is the social ($\vec{r}_2 * c_2 (\vec{g}_i(t) - \vec{x}_i(t))$), being the same as the previous one, but considering the distance from the position of the particle to the global historical maximum of all.

Applying the PSO algorithm to the cost optimization problem with 30 particles and 20 iterations, the evolution of these particles both individually and collectively is observed as shown in Figures 7 and 8.

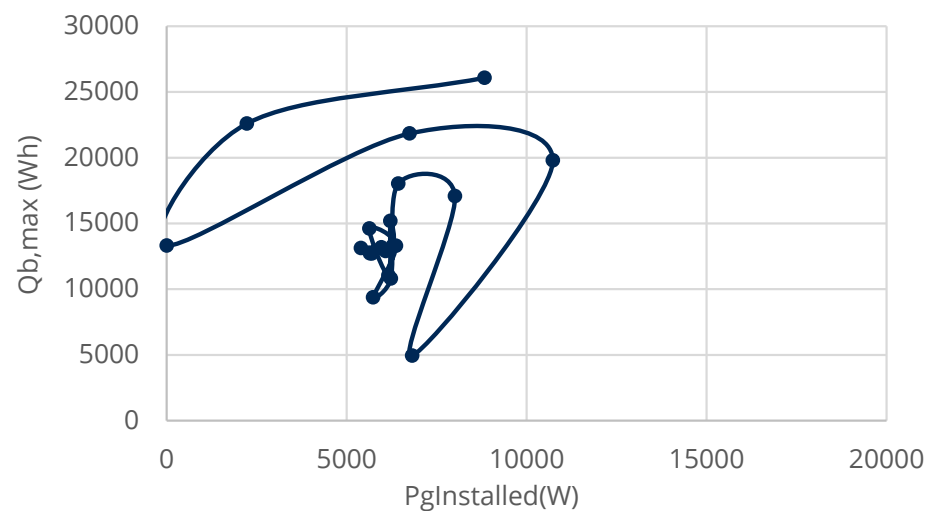


Figure 7. Trajectory of a particle throughout the optimization process.

Not all the particles end at the same point; this is because the algorithm ends before they have had time to reach the optimum. Likewise, this is independent of the operation of the algorithm since, being initially uniformly distributed in space, the particles closest to the optimum manage to find the solution satisfactorily (Figure 9).

One advantage of this algorithm is that, since it is approximate and without discretization, it allows a much lower number of iterations to be used in the Monte Carlo simulation, since the error that can be made in the calculation of the system will be negligible when the solution is discretized and opts for commercially available power and capacity to make up the system. Thus, a total of 100 iterations have been used in the Monte Carlo simulation to obtain the averaged results (Figure 10).

The global objective function of the system remains almost constant in this method, since, with a sufficiently large population, a system close to the optimum will already be found in the first iteration, while if we observe the evolution of a particular particle, its objective function will oscillate and attenuate as it approaches the optimum.

Based on the literature analysis, the decision to use the PSO algorithm for this research was based on several key factors. Firstly, PSO allows the analysis of cost and reliability simultaneously. This makes it suitable for a complex problem with conflicting objectives. Secondly, PSO's global optimization capabilities are vital for efficiently exploring a wide parameter space in the presented problem domain. Thirdly, its relatively fast convergence aligns with the practical engineering applications, considering computational time constraints in sizing stand-alone photovoltaic (SAPV) systems. Additionally, PSO's adaptability allows customization to match the specific constraints and objectives of the studied SAPV system-sizing problem. Lastly, its extensive use in both academia and industry provided a

strong foundation for its applicability to the presented research, making it the ideal choice among various optimization techniques.

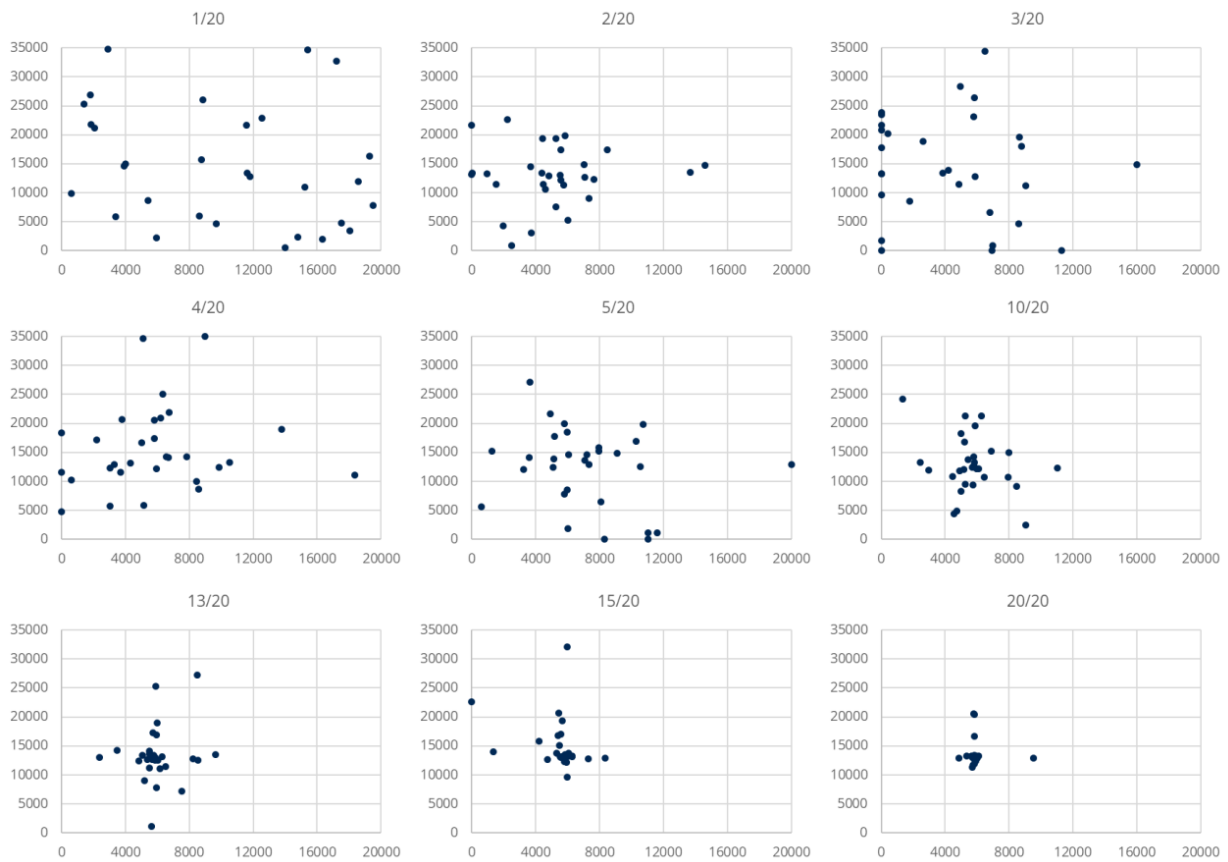


Figure 8. Position of the particles throughout the optimization process.

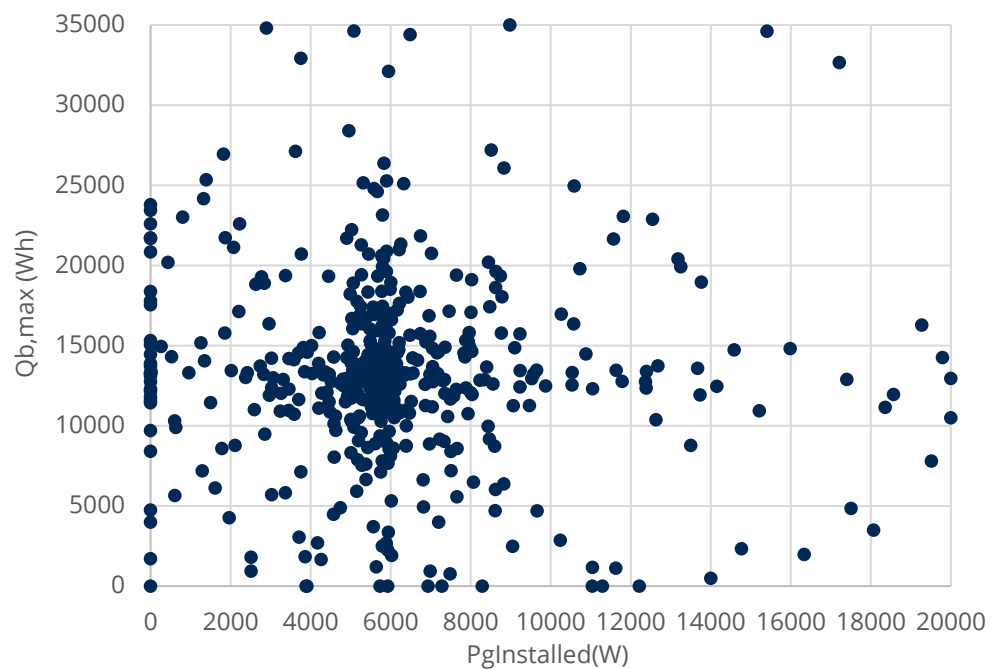


Figure 9. Totality of positions explored in the optimization process.

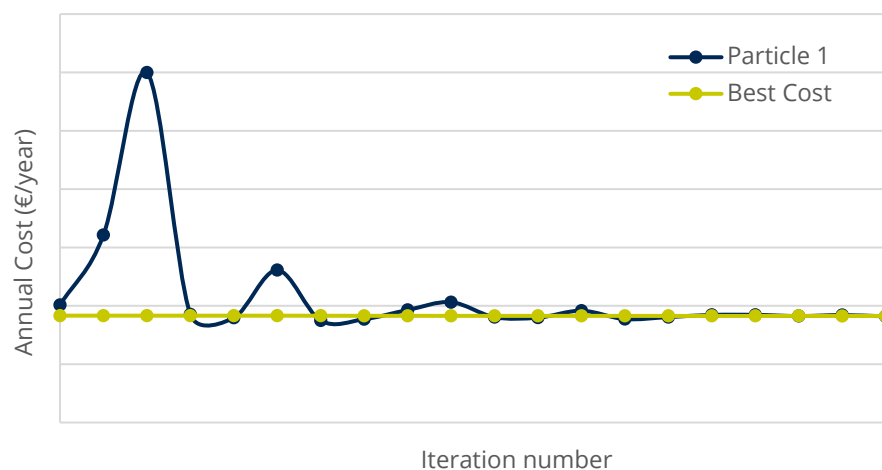


Figure 10. Evolution of the objective function for a particle and the global absolute.

3. Results

In this section, the performance of the PSO optimization algorithm is evaluated and then it is applied to a case study for the optimal design of an SAPV system.

3.1. Validation of the Cost Optimization Method

To contrast the results obtained by the PSO optimization algorithm, they are compared with the results obtained from an iterative heuristic optimization of the SAPV system design based on discrete increases and decreases in the installed PV power and battery storage capacity. The heuristic algorithm followed for the iterative optimization of the SAPV system is the one shown in Figure 11.

Each candidate solution consists of:

- Candidate 1: Discreet increase in PV power.
- Candidate 2: Discreet increase in battery capacity.
- Candidate 3: Discrete decrease in PV power.
- Candidate 4: Discreet decrease in battery capacity.

The optimal improvement is chosen as the one that minimizes the cost of the installation among the four tested options. If this does not improve with respect to the system established in the previous optimization iteration, the algorithm concludes that it has reached the optimal solution.

The solution found, the optimization time of the PSO optimization algorithm, and the discrete heuristic optimization procedure have been compared. In the first place, the solution reached in both methods is the same, showing that both converge equally for the same installed PV power and installed battery capacity (Figure 12).

In the PSO algorithm, some points do not get to group with the rest at the optimal value in the established simulation time due to the lack of iterations. These values are typically the ones that were originally furthest from the optimal solution. The points that are not directly in the optimum will not affect the solution delivered by the method, since it is considered the best of each series.

The simulation time is a difficult parameter to compare between the two methods, since while the PSO algorithm always performs the same number of operations given that the number of iterations and systems (particles) is predefined, the iterative heuristic method starts from an initial system that may be closer or further from the final solution, and the number of operations to perform will vary with it (Figure 13). The data collected for some of the simulations carried out in the previous sections are shown in Table 1.

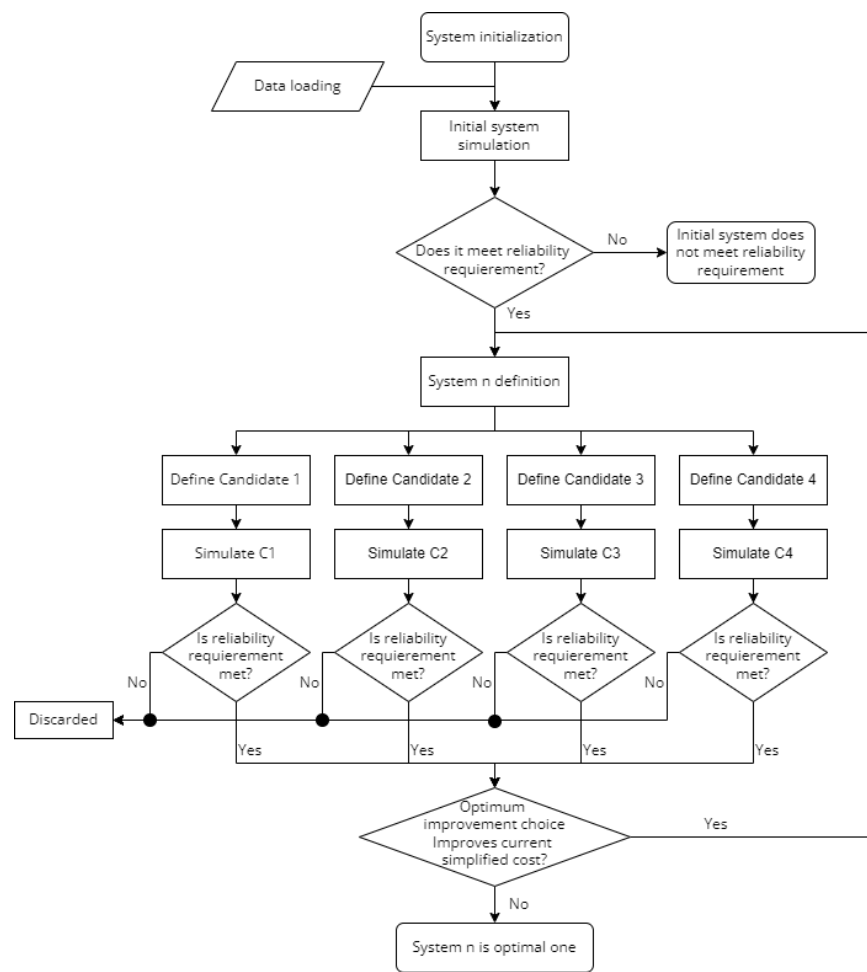


Figure 11. Iterative process of discrete optimization of the SAPV system.

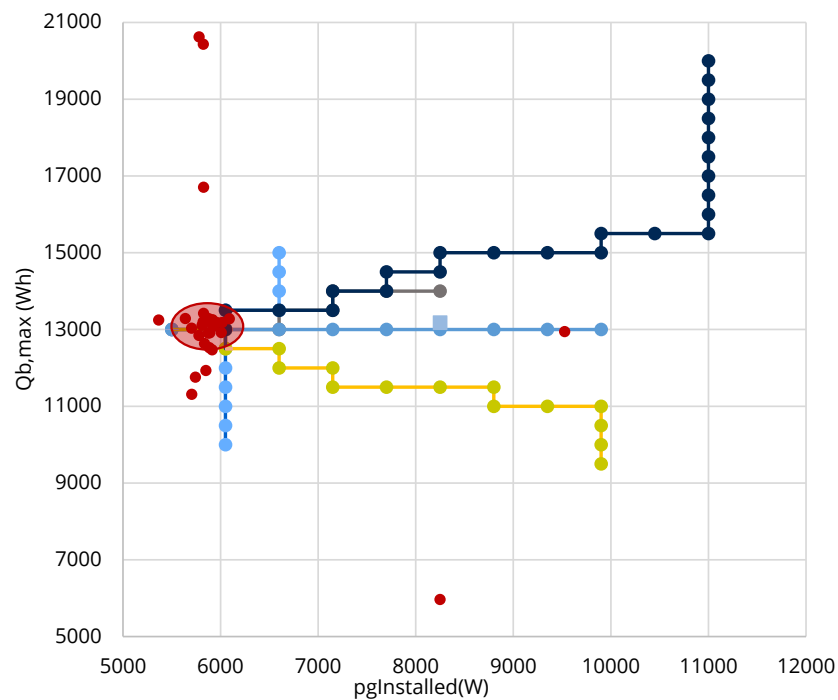


Figure 12. Convergence of the PSO method (red points) and heuristic method (rest of points for different initial values).

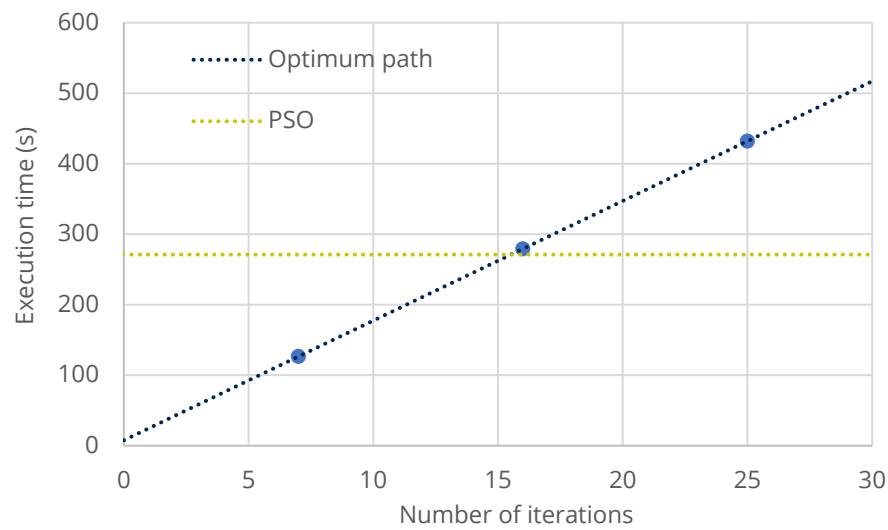


Figure 13. Simulation time versus iterations of the optimization algorithm.

Table 1. Optimization method comparison.

Method 1: Heuristic optimization process					
InitialPgInstalled (W)	Initial Qb,max (Wh)	EndPgInstalled (W)	Final Qb,max (Wh)	Time(s)	Total iterations
6050	10,000	6050	13,000	126.5	7
9900	9500	6050	13,000	279.2	16
11,000	20,000	6050	13,000	432.0	25
Method 2: PSO algorithm					
InitialPgInstalled (W)	Initial Qb,max (Wh)	EndPgInstalled (W)	Final Qb,max (Wh)	Time(s)	Total iterations
-	-	5778.57	12,845.35	271.0	-

3.2. SAPV System Case Study

In order to evaluate the proposed design method, an installation located at the Energy Engineering Institute of the UPV [48] is considered for a typical demand of a house with a power demand of up to 4.6 kW. The most recent PVGIS irradiance data for the year 2020 have been taken. The parameters considered for this case study are shown in Table 2.

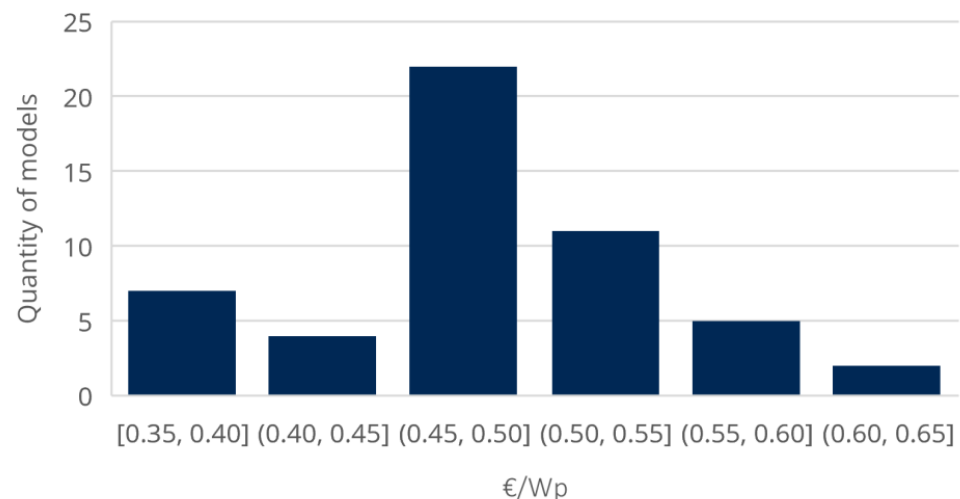
The price of the regulator for the installation is not considered since a combined inverter with a regulator oriented to PV installations has been chosen for the study. Several of these inverters can work in parallel to support the power of the installation. The performance and other technical parameters, as well as the prices, have been obtained either from the technical datasheets of this equipment, from market analysis, directly from the distributor, or from documents from recognized institutions [49,50]. The power of the PV modules and the nominal capacity of the battery modules are used for the discretization of the results. The generator consumption has been estimated from the power produced and the fuel consumption at a 75% load.

To determine the data to be entered into the reliability simulator and optimizer, a study has been carried out where data have been collected from four local distributors and one national distributor of photovoltaic modules and batteries for these systems.

Data have been obtained for five of the ten largest capacity PV module manufacturers in the world [51]. In order to normalize the different technologies of each manufacturer and the nominal generation power of the panel, the price of each module has been normalized by dividing it by its nominal power and finding the weighted average of all the modules collected, for a total of 51 modules (Figure 14). An average price with a VAT of 0.488 EUR/Wp (0.403 EUR/Wp without VAT) has been obtained.

Table 2. SPAV case study system parameters.

Battery charging efficiency	0.93		SPF-5000-ES
Battery discharging efficiency	0.93		SPF-5000-ES
Required reliability	90	%	
Rated power	550	W	JAM72S30-550
Ktemp power	−0.35	%	JAM72S30-550
Rated capacity	3552	Wh	Pylontech US3000C
Pdmax	4600	W	
PV power price	0.488	EUR/W installed	
PV life	25	Years	JAM72S30-550
Battery capacity price	0.597	EUR/Wh installed	
Battery life	15	Years	Pylontech US3000C
Inverter price	665	EUR	SPF-5000-ES (unitary price)
Regulator price	0	EUR	Combined in inverter
Diesel consumption cost	0.6	l/kWh	Genergy Aneto 75% charge
Fuel price	1878	EUR/l	Gasoline

**Figure 14.** Quantity of module models per normalized price range.

A similar procedure has been followed for batteries. Currently, there are different battery technologies with different characteristics that are used for self-consumption systems. The main technologies are lead acid, AGM, GEL and lithium (LFP lithium steel phosphate), which are being introduced due to their progressive price reduction. Assessing the differences between different technologies [52] and given its stability in maintaining the charge and discharge voltage, its low maintenance, its suitability for deep cycle applications, and its progressive decrease in price, LFP technology has been chosen. The developed method also allows consideration of data for batteries from other technologies that could be used in the installation.

The procedure followed was similar to the previous one, taking data from different distributors for the main lithium battery models, for a total of 120 items, obtaining an average price with a VAT of 0.597 EUR/Wh (0.493 EUR/Wh without VAT) (Figure 15).

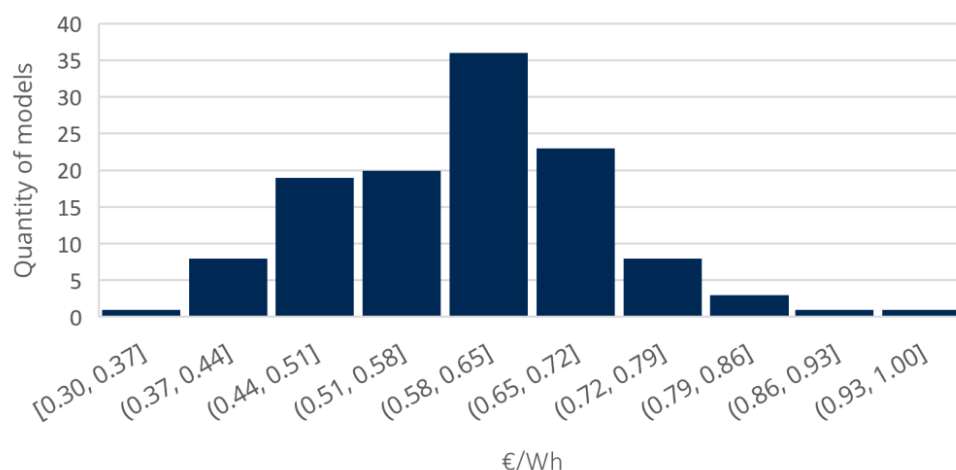


Figure 15. Quantity of battery models per normalized price range.

The results obtained from the optimization of an SAPV system with the data referred to above and for each of the methods developed are shown in Table 3.

Table 3. Results of the design optimization of the SAPV system for 2020 climatological data.

	Iterative Heuristic Algorithm	Continuous PSO Algorithm	Discretized PSO
Installed power (W)	9900	9525	9900
Battery capacity (Wh)	17,760	17,668	17,760
Reliability (%)	93.78	93.65	93.65
Approximate annual cost (EUR/year)	1828.24	1825.99	1828.79

In this case, when discretizing the PSO algorithm, the convergence of the results obtained is observed. This solution translates into 9900 W in PV modules and a rack with five 3550 Wh batteries.

4. Discussion

In order to verify the variation in the results with the variation in the input data, a sensitivity study is carried out taking different parameters into account.

4.1. Climatological Year

First, the variation in the optimal system will be verified depending on the year used in the climatology data extracted from the PVGIS database. It is carried out for the records from 2015 to 2019, comparing them with the previous results for the year 2020 (Table 4). In all of them, the installation presents the same characteristics, and it is assumed that the market prices are the same.

It can be seen in Figure 16 that there are differences in the results. Although the ideal battery capacity is not affected, the necessary installed power does vary by up to 2750 W in the discretized calculations (corresponding to five modules). The interpretation of this may be due to a greater or lesser concentration of days of low PV production (cloudy or rainy days) at times of the year with lower irradiance. With the same energy storage capacity, it is possible to supply the demand in this period. A greater frequency of these low PV production days implies greater installed PV power to be able to store enough energy.

Table 4. Optimal system depending on the year.

	2015		2016		2017		2018		2019		2020	
	C.Opt	PSO										
P_{inst} (W)	9350	9017	11,550	11,409	10,450	10,545	9900	9436	8800	9147	9900	9350
Capacity (Wh)	17,760	17,998	17,760	17,140	17,760	17,623	17,760	18,125	17,760	17,849	17,760	17,668
Reliability (%)	94.40	94.59	93.65	93.06	94.13	94.07	93.69	93.98	93.8	94.02	93.78	93.65
EUR/year	1765.1	1761.6	1881.1	1875.3	1821.5	1817.1	1833.5	1830.7	1807.1	1803.3	1828.2	1826.0
EUR/kWh	4.38	4.41	4.45	4.38	4.37	4.36	4.41	4.47	4.39	4.39	4.41	4.41

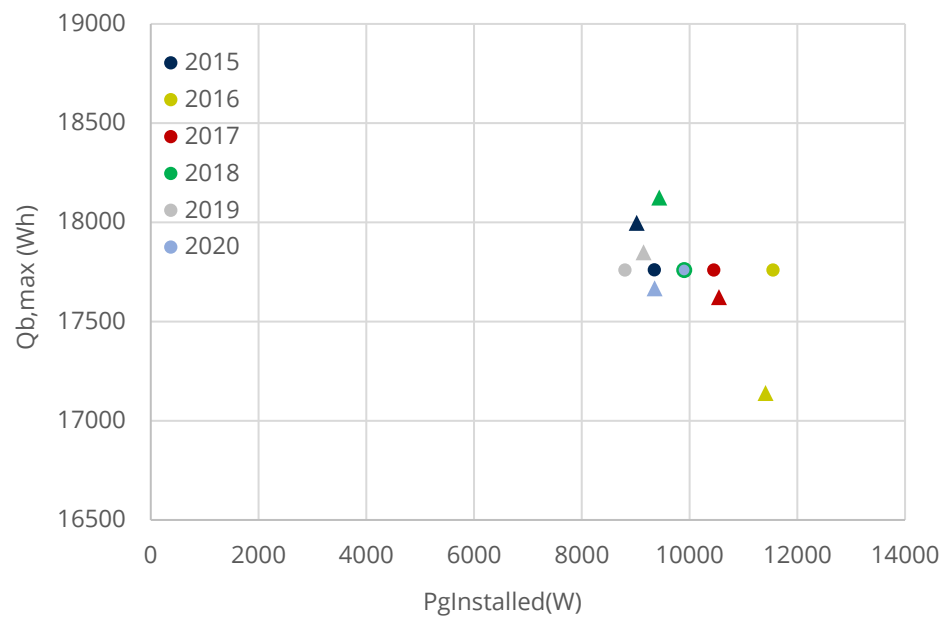


Figure 16. Optimal solution depending on the year studied (circle: heuristic method; triangle: PSO).

Taking information from AEMET [53], the reason for these variations can be analyzed from the data represented in Figures 17 and 18.

The data have been taken from the datosclima.es website (accessed on 10 October 2023), which obtains the data directly from the AEMET OpenData API (https://www.aemet.es/en/datos_abiertos/AEMET_OpenData) (accessed on 10 October 2023), which has national climatological data records available to any user. The data have been taken for the closest weather station to the location of the SAPV installation (Table 5).

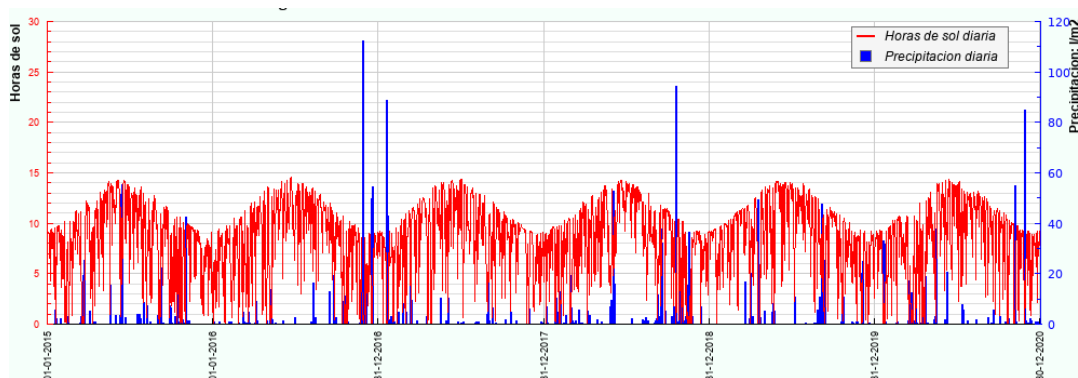


Figure 17. Historic precipitation and solar hours at Valencia Airport 2015–2020.

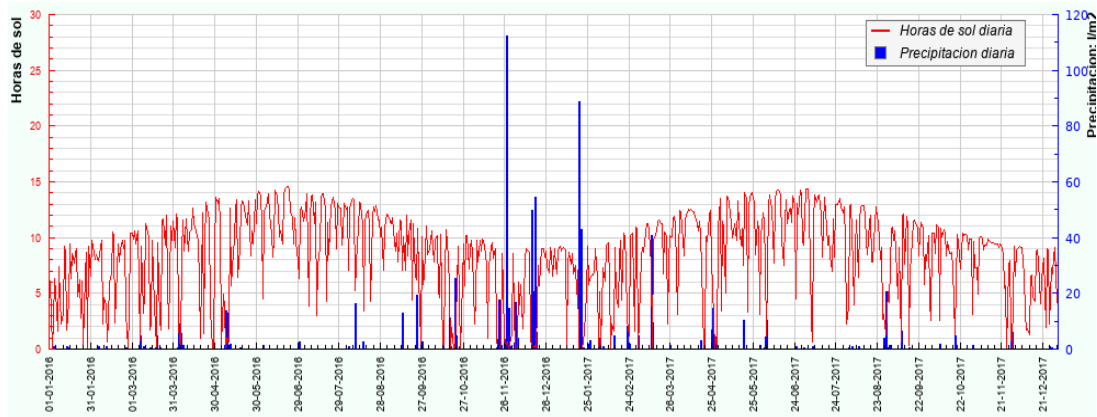


Figure 18. Historical precipitation and solar hours in the area of interest in the years 2016–2017.

Table 5. Accumulated hours of sunshine per year recorded in the area of interest.

Year	Cumulative Sun Hours
2015	2991.7
2016	2963.2
2017	3158.0
2018	3010.2
2019	3161.9
2020	3013.3

It can be seen that 2016 is the year with the fewest hours of sunshine among those analyzed. This, although not conclusive, gives clues as to why this is the year that presents an optimal system with greater power compared to the rest, although it disagrees with the fact that 2017 is the year with the highest installed power, being one of the years that more solar hours were accumulated. Next, if we pay attention to the distribution of solar hours in Figure 18, a prolonged period of lower radiation is observed in both, which explains this fact.

In both years, there is a prolonged period of lower solar incidence, with brief peaks that are in line with the average for the time. This temporary distribution explains the profitability of a greater installed capacity to cover the cost of fuel consumption in those specific periods.

In the case of having the calculations for all the years, the solution for 2016 would be the one to apply; however, the system provided in 2020 is a compromise solution between all of them. Another solution would be to take the data for the TMY in PVGIS and convert them to the desired inclined plane, although this solution would also give an averaged system.

Comparing the optimal system for each year with the meteorological data of 2016, these being the most critical among those analyzed, the reliability parameters obtained are shown in Table 6.

Table 6. Reliability of the optimal system for each year for 2016 data.

Year	Power Installed (W)	Battery Capacity (Wh)	Reliability (%)
2015	9350	17,760	92.97
2016	11,550	17,760	93.65
2017	10,450	17,760	93.35
2018	9900	17,760	93.17
2019	8800	17,760	92.73
2020	9900	17,760	93.17

As can be seen, although the optimal system varies from year to year since it is optimized for the minimum cost, which is very sensitive to the hours not supplied where a secondary generator has had to act, the system’s supply reliability, once it is in the order of magnitude of the optimum, is quite insensitive to small variations in the installed power, fulfilling the technical requirement of reliability.

4.2. Price of Components and Fuel

In the calculation of costs, three price parameters are involved—that of the photovoltaic modules, that of the batteries, and that of the fuel to make up for the deficit in solar generation. These three prices tend to change in the short to medium term, so it is interesting to study how the optimal system varies with them.

First, the system is analyzed with the variation in the price of PV modules, which have suffered a significant price decrease in the last decade (Figure 19).

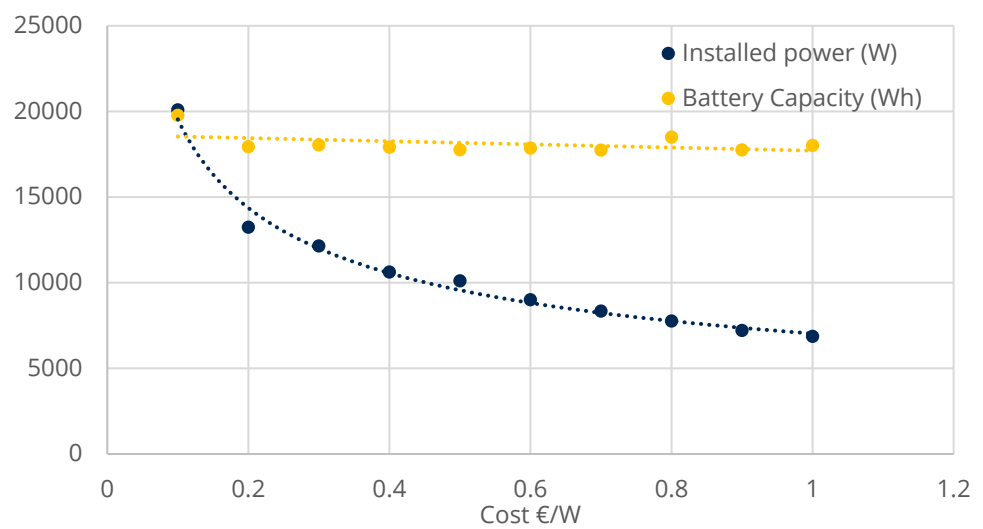


Figure 19. Variation of power and optimal capacity with the price of PV modules.

As seen in Figure 19, the optimal storage capacity is not affected by the price of the modules. As expected, the optimal installed power increases as the price decreases. From these data, a better conclusion can be drawn from Figure 20.

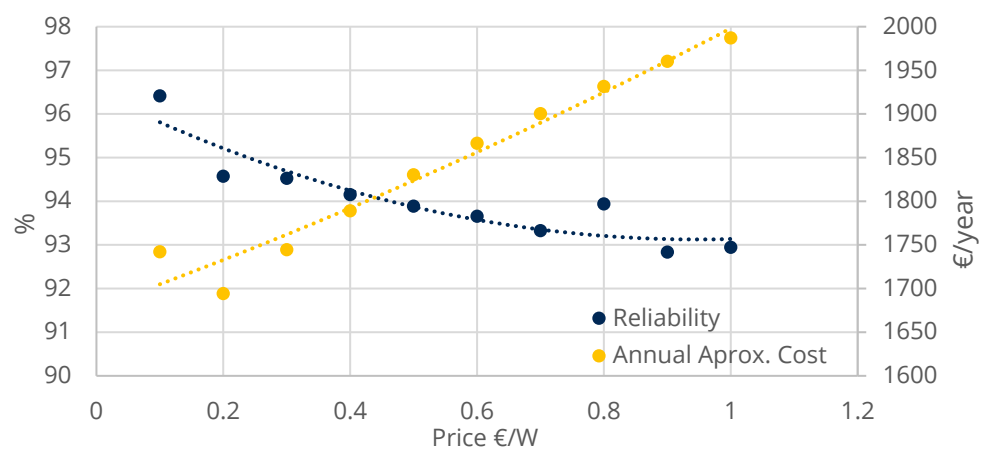


Figure 20. Variation of power and optimal capacity with the price of the modules.

The reliability of the system increases with the decrease in the price of the panels, for which reason, having a very oversized installation power to charge the battery enough to

fully supply the periods of lower generation and eliminate the cost of fuel consumption is prioritized.

Analyzing the evolution of the system and setting all the parameters except the price of battery storage, a similar effect is observed (Figure 21).

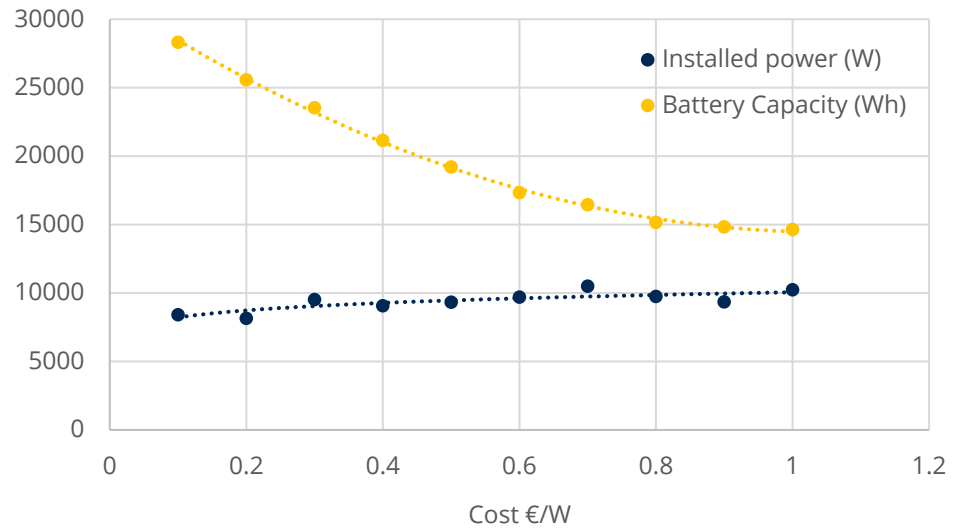


Figure 21. Variation of the power and optimal capacity with the price of the batteries.

Installed power remains practically constant, decreasing slightly as storage capacity increases. Meanwhile, storage capacity skyrockets for low storage prices, increasing supply reliability (Figure 22).

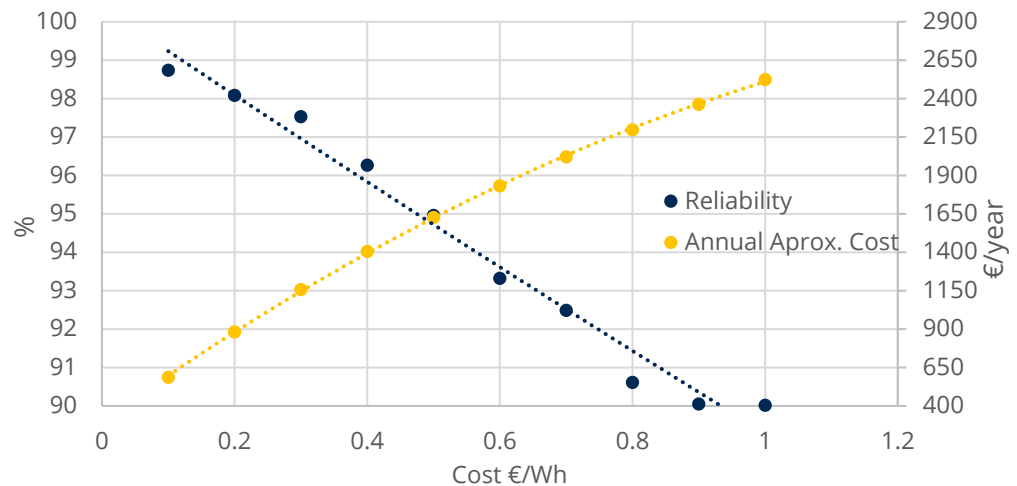


Figure 22. Variation of the reliability and cost of the system with the price of the batteries.

In this case, the difference is even more exaggerated, since an equal percentage variation in the price of the batteries is much more significant than in the case of PV modules, making the need for a secondary generator practically zero when the price is cheaper. Given current prices (approx. 0.5 EUR/W for PV modules and 0.6 EUR/Wh for batteries), a USD 0.1 decrease in batteries would produce approximately a 1.5% increase in reliability and a EUR 200 decrease in cost system, while the same variation in PV modules would produce only a 0.2% improvement in reliability and less than EUR 50 decrease in cost, concluding that the price of energy storage is much more significant in the system.

Finally, the same analysis is conducted for the price of fuel, which generally fluctuates more frequently than component prices (Figure 23).

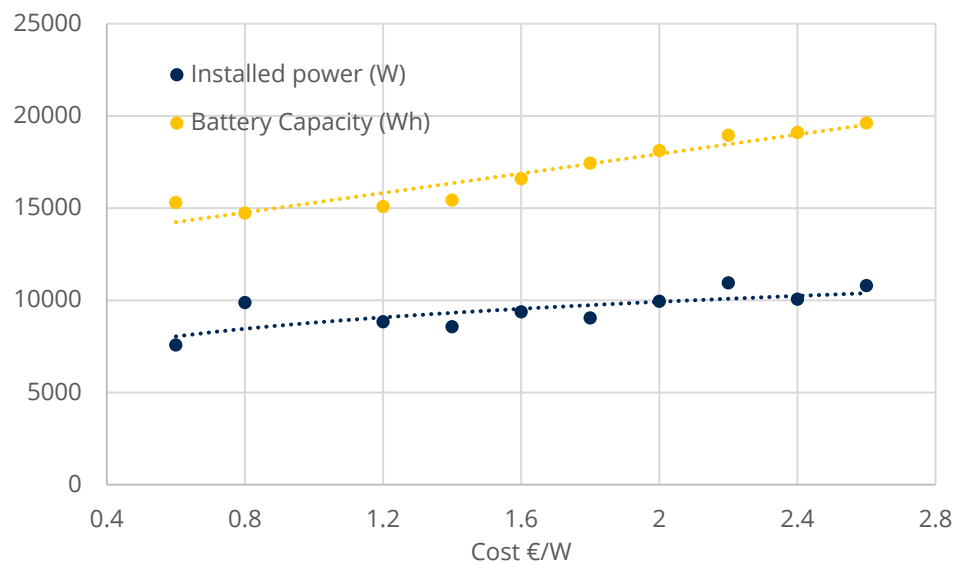


Figure 23. Optimum power and capacity variation with fuel price.

It can be seen in Figure 23 how a price increase gives rise to an identical reaction in the two main components of the system, increasing installed power and storage capacity, with the consequent increase in supply reliability and annual cost (Figure 24).

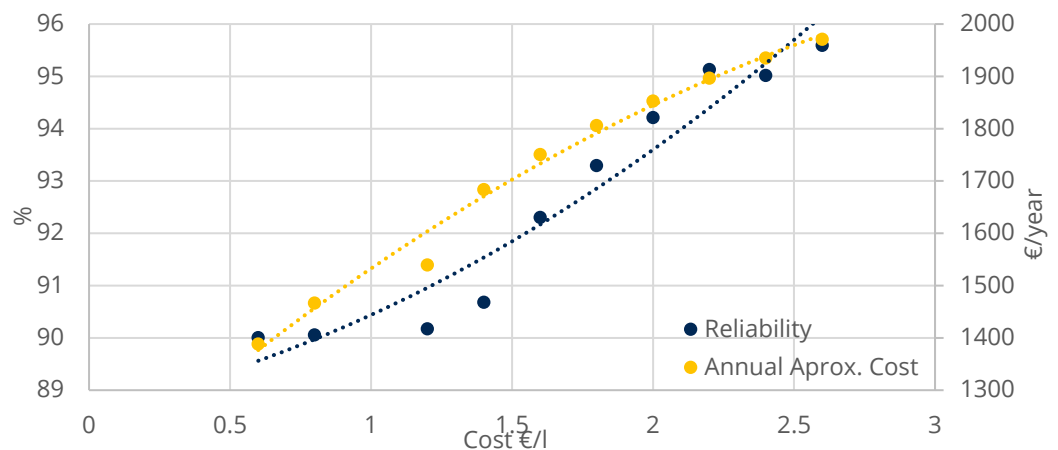


Figure 24. Variation of the reliability and cost of the system with the price of fuel.

Inevitably, an increase in the cost of fuel has an equal reflection on the total cost of the installation. The cost of increasing the power and capacity of the system without fuel is less than the increase in the cost of fuel to cover the hours of solar supply failure, but it also translates into an increase in the total cost. Regardless of this study, if macroeconomic effects are considered, an increase in the price of fuel may cause an increase in the price of the rest of the products, modifying the trend curves previously seen.

5. Conclusions

The developed PSO optimization method allows a high degree of flexibility in the calculation of the optimal SAPV installation. The methodology that performs the optimal system sizing allows the collection of irradiance log data for any location and its use in the system calculation, as well as the input of detailed demand profiles. It also allows the input of parameters for specific commercial PV components, making the system solution unique and optimal for each individual user.

The PSO optimization method always converges to the same result, having used two different optimization algorithms to corroborate this fact and check the accuracy of the result. This fact, together with the computational speed of the algorithms, is sufficient to admit the feasibility of using the program in the design of larger SAPV systems.

Sensitivity analysis of the annual irradiance data indicates that, once the optimal system has been obtained in the indicated order of magnitude, the system solution allows for a margin of error while maintaining the desired supply reliability.

Looking at the trends and price sensitivity analyses, it can be concluded that the trend for these mixed off-grid systems, which combine photovoltaics with an external generator, is towards a pure photovoltaic system. The market trend is towards lower costs for both PV modules and batteries, so the system will evolve towards the elimination of the auxiliary generator in favor of increasing the installed power and, above all, the storage capacity, thus increasing the reliability of supply to values close to 100%.

Finally, it should be added that, although a fully functional design method has been obtained, it can be improved in future work, allowing for improvements in the installation calculation model, taking into account, for example, maintenance costs and replacement of the components of the system, and the effect of aging on these system components, which would affect both their failure rate and the generation capacity of the PV modules and the storage capacity of the batteries.

It can be concluded that this research makes a significant contribution to the field by providing a complete and robust study that addresses various critical aspects of SAPV system design.

Author Contributions: Conceptualization, E.Q.-C., A.M.-T., C.R.-P. and C.R.-B.; methodology, A.M.-T., E.Q.-C. and C.R.-B.; software, A.M.-T. and C.R.-B.; validation, E.Q.-C., A.M.-T. and C.R.-P.; formal analysis, A.M.-T. and E.Q.-C.; research, E.Q.-C., A.M.-T., C.R.-B. and C.R.-P.; resources, E.Q.-C., A.M.-T. and C.R.-B.; data curation, A.M.-T.; writing—original draft preparation, A.M.-T. and E.Q.-C.; writing—review and editing, A.M.-T., E.Q.-C., C.R.-B. and C.R.-P.; visualization, E.Q.-C., A.M.-T. and C.R.-P.; supervision, E.Q.-C., C.R.-P. and C.R.-B.; project administration, E.Q.-C., C.R.-B. and C.R.-P.; funding acquisition, E.Q.-C., C.R.-B. and C.R.-P. All authors have read and agreed to the published version of the manuscript.

Funding: Vicerrectorado de Investigación de la Universitat Politècnica de València (PAID-11-22).

Institutional Review Board Statement: Not applicable.

Informed Consent Statement: Not applicable.

Data Availability Statement: Not applicable.

Acknowledgments: This work has been supported by Universitat Politècnica de València.

Conflicts of Interest: The authors declare no conflict of interest.

Abbreviations

AC	Alternating current.
BC	Battery controller.
DC	Direct current.
DN	Distribution network.
E_b	Energy contributed by the battery.
E_d	Daily energy consumption.
E_1	Excess energy produced by the photovoltaic panels.
ENU	Energy not used.
FOI	Frequency of interruptions.
GCS	Generating capacity sequence.
HRES	Hybrid renewable energy systems.
LOEE	Loss of energy expectation index.
LOLP	Loss of load probability index.

LOLE	Loss of load expectation index.
LOPE	Loss of power expectation index.
MCS	Monte Carlo simulation.
n_c	Consecutive cloudy days.
$P_d(t)$	Instantaneous power demand.
$P_{d(\text{peak})}$	Maximum demanded power.
PNU	Power not used.
PSO	Particle Swarm Optimization.
PV_{peak}	Rated power installed in the photovoltaic panels.
$P_S(t)$	Power produced by the photovoltaic array.
PV	Photovoltaic array generation system.
Q_b	Battery capacity.
SAPV	Stand-alone photovoltaic system.
SOC	State of charge of battery.
SOC_{max}	Maximum admissible value of SOC.
SOC_{min}	Minimum admissible value of SOC.
TTF	Time to failure.
TTR	Time to repair.
λ_b	Battery failure rate per year.
λ_c	Photovoltaic panel array and battery controller failure rate per year.
λ_i	Inverter failure rate per year.
η_b	Li-ion battery efficiency.
η_c	Battery charging efficiency.
η_d	Battery discharging efficiency.

References

- Twaha, S.; Ramli, M.A.M. A review of optimization approaches for hybrid distributed energy generation systems: Off-grid and grid-connected systems. *Sustain. Cities Soc.* **2018**, *41*, 320–331. [CrossRef]
- IEA PVPS. *Trends 2018 in Photovoltaic Applications*; T1-34:2018; IEA PVPS: Paris, France, 2018. Available online: http://www.iea-pvps.org/fileadmin/dam/intranet/task1/IEA_PVPS_Trends_2018_in_Photovoltaic_Applications.pdf (accessed on 3 February 2020).
- Ahmed, R.; Basit, A.; Abid, Q.u.D.; Haroon, M.; Kakar, F.; Ullah, N.; Khan, D.A. Techno-Economic Investigation of Standalone Photovoltaic Energy Systems for Rural Areas of Quetta. *Eng. Proc.* **2023**, *45*, 30. [CrossRef]
- Masson, G.; Latour, M. Self-consumption as the new Holy Grail of the PV industry: From theory to reality. In *Photovoltaics International*, 17th ed.; PV Tech: London, UK, 2012; pp. 166–169.
- Mandelli, S.; Barbieri, J.; Mereu, R.; Colombo, E. Off-grid systems for rural electrification in developing countries: Definitions, classification and a comprehensive literature review. *Renew. Sustain. Energy Rev.* **2016**, *58*, 1621–1646. [CrossRef]
- Luthander, R.; Widen, J.; Nilsson, D.; Palm, J. Photovoltaic self-consumption in buildings: A review. *Appl. Energy* **2015**, *142*, 80–94. [CrossRef]
- Evans, A.; Strezov, V.; Evans, T.J. Assessment of utility energy storage options for increased renewable energy penetration. *Renew. Sustain. Energy Rev.* **2012**, *16*, 4141–4147. [CrossRef]
- Bugala, A.; Zaborowicz, M.; Boniecki, P.; Janczak, D.; Koszela, K.; Czekala, W.; Lewicki, A. Short-term forecast of generation of electric energy in photovoltaic systems. *renew. Sustain. Energy Rev.* **2018**, *81 Pt 1*, 306–312. [CrossRef]
- Abuagreb, M.; Allehyani, M.; Johnson, B.K. Design and Test of a Combined PV and Battery System under Multiple Load and Irradiation Conditions. In Proceedings of the 2019 IEEE Power & Energy Society Innovative Smart Grid Technologies Conference (ISGT), Washington, DC, USA, 17–20 February 2019; pp. 1–5. [CrossRef]
- Moharil, R.M.; Kulkarni, P.S. Reliability analysis of solar photovoltaic system using hourly mean solar radiation data. *Sol. Energy* **2010**, *84*, 691–702. [CrossRef]
- Dissawa, D.M.H.L.; Godaliyadda, G.M.R.I.; Ekanayake, M.P.B.; Ekanayake, J.B.; Agalgaonkar, A.P. Cross-correlation based cloud motion estimation for short-term solar irradiation predictions. In Proceedings of the 2017 IEEE International Conference on Industrial and Information Systems (ICIIS), Peradeniya, Sri Lanka, 15–16 December 2017; pp. 1–6. [CrossRef]
- Kaplani, E.; Kaplanis, S. A stochastic simulation model for reliable PV system sizing providing for solar radiation fluctuations. *Appl. Energy* **2012**, *97*, 970–981.
- Benmouiza, K.; Tadj, M.; Cheknane, A. Classification of hourly solar radiation using fuzzy c-means algorithm for optimal stand-alone PV system sizing. *Int. J. Electr. Power Energy Syst.* **2016**, *82*, 233–241. [CrossRef]
- Ozogwu, C.G. Artificial neural network forecast of monthly mean daily global solar radiation of selected locations based on time series and month number. *J. Clean. Prod.* **2019**, *216*, 1–13. [CrossRef]
- Palensky, P.; Dietrich, D. Demand Side Management: Demand Response, Intelligent Energy Systems, and Smart Loads. *IEEE Trans. Ind. Inform.* **2011**, *7*, 381–388. [CrossRef]

16. Roldan-Blay, C.; Escrivá-Escrivá, G.; Roldán-Porta, C. Improving the benefits of demand response participation in facilities with distributed energy resources. *Energy* **2019**, *169*, 710–718. [CrossRef]
17. Goel, S.; Sharma, R. Performance evaluation of stand alone, grid connected and hybrid renewable energy systems for rural application: A comparative review. *Renew. Sustain. Energy Rev.* **2017**, *78*, 1378–1389. [CrossRef]
18. Weniger, J.; Tjaden, T.; Quaschnig, V. Sizing of residential PV battery systems. *Energy Procedia* **2014**, *46*, 78–87. [CrossRef]
19. Maleki, A.; Rosen, M.; Pourfayaz, F. Optimal operation of a grid-connected hybrid renewable energy system for residential applications. *Sustainability* **2017**, *9*, 1314. [CrossRef]
20. Cao, S.; Hasan, A.; Sirén, K. Matching analysis for on-site hybrid renewable energy systems of office buildings with extended indices. *Appl. Energy* **2014**, *113*, 230–247. [CrossRef]
21. Ren, H.; Wu, Q.; Gao, W.; Zhou, W. Optimal operation of a grid-connected hybrid PV/fuel cell/battery energy system for residential applications. *Energy* **2016**, *113*, 702–712. [CrossRef]
22. Ghafoor, A.; Munir, A. Design and economics analysis of an off-grid PV system for household electrification. *Renew. Sustain. Energy Rev.* **2015**, *42*, 496–502. [CrossRef]
23. Maleki, A.; Hajinezhad, A.; Rosen, M.A. Modeling and optimal design of an off-grid hybrid system for electricity generation using various biodiesel fuels: A case study for Davarzan, Iran. *Biofuels* **2016**, *7*, 669–712. [CrossRef]
24. Castillo-Cagigal, M.; Caamano-Martin, E.; Matallanas, E.; Dough-Bote, D.; Gutierrez, A.; Monasterio-Huelin, F.; Jiménez-Leube, J. PV self-consumption optimization with storage and Active DSM for the residential sector. *Sol. Energy* **2011**, *85*, 2338–2348. [CrossRef]
25. Zhou, W.; Lou, C.; Li, Z.; Lu, L.; Yang, H. Current status of research on optimum sizing of stand-alone hybrid solar–wind power generation systems. *Appl. Energy* **2010**, *87*, 380–389. [CrossRef]
26. Yadav, A.K.; Chandel, S.S. Solar radiation prediction using Artificial Neural Network techniques: A review. *Renew. Sustain. Energy Rev.* **2014**, *33*, 772–781. [CrossRef]
27. JPW Stackhouse. Surface meteorology and Solar Energy. Atmospheric Science Data Center. 2011. Available online: <https://eosweb.larc.nasa.gov/> (accessed on 3 February 2020).
28. Roldan-Blay, C.; Escrivá-Escrivá, G.; Roldan-Porta, C.; Álvarez-Bel, C. An optimization algorithm for distributed energy resources management in micro-scale energy hubs. *Energy* **2017**, *132*, 126–135. [CrossRef]
29. Hoevenaars, E.J.; Crawford, C.A. Implications of temporal resolution for modeling renewable-based power systems. *Renew. Energy* **2012**, *41*, 285–293. [CrossRef]
30. Cao, S.; Sirén, K. Impact of simulation time-resolution on the matching of PV production and household electric demand. *Appl. Energy* **2014**, *128*, 192–208. [CrossRef]
31. Cucchiella, F.; D’Adamo, I.; Gastaldi, M.; Stornelli, V. Solar Photovoltaic Panels Combined with Energy Storage in a Residential Building: An Economic Analysis. *Sustainability* **2018**, *10*, 3117. [CrossRef]
32. Kosmadakis, I.E.; Elmasides, C.; Eleftheriou, D.; Tzagarakis, K.P. A Techno-Economic Analysis of a PV-Battery System in Greece. *Energies* **2019**, *12*, 1357. [CrossRef]
33. Werner, C.; Breyer, C.; Gerlach, A.; Beckel, O. Photovoltaic with Energy Storage: An Overview on Economics, System Design and Politics. In Proceedings of the 27th European Photovoltaic Solar Energy Conference, Frankfurt, Germany, 24–28 September 2012.
34. Faza, A. A probabilistic model for estimating the effects of photovoltaic sources on the power systems reliability. *Reliab. Eng. Syst. Saf.* **2018**, *171*, 67–77. [CrossRef]
35. Borges, C.L.T. An overview of reliability models and methods for distribution systems with renewable energy distributed generation. *Renew. Sustain. Energy Rev.* **2012**, *16*, 4008–4015. [CrossRef]
36. Billinton, R. Reliability considerations in the utilization of wind energy, solar energy and energy storage in electric power systems. In Proceedings of the 2006 International Conference on Probabilistic Methods Applied to Power Systems, Stockholm, Sweden, 11–15 June 2006; IEEE: Piscataway, NJ, USA, 2006; pp. 1–6.
37. Elbeltagi, E.; Hegazy, T.; Grierson, D. Comparison among five evolutionary-based optimization algorithms. *Adv. Eng. Inform.* **2005**, *19*, 43–53. [CrossRef]
38. Kachitvichyanukul, V. Comparison of three evolutionary algorithms: GA, PSO, and DE. *Ind. Eng. Manag. Syst.* **2012**, *12*, 215–223. Available online: https://www.academia.edu/5001982/Comparison_of_Three_Evolutionary_Algorithms_GA_PSO_and_DE (accessed on 10 October 2023). [CrossRef]
39. El-Ghandour, H.; Elbeltagi, E. Comparison of Five Evolutionary Algorithms for Optimization of Water Distribution Networks. *J. Comput. Civ. Eng.* **2018**, *32*, 04017066. [CrossRef]
40. Heris, M.K. Particle Swarm Optimization in MATLAB. (Yarpiz). 2015. Available online: <https://yarpiz.com/50/ypea102-particle-swarm-optimization> (accessed on 6 June 2023).
41. Joint Research Center—European Commission. PVGIS Tool. Available online: https://re.jrc.ec.europa.eu/pvg_tools/en/ (accessed on 28 May 2023).
42. Eltawil, M.A.; Zhao, Z. Grid-connected photovoltaic power systems: Technical and potential problems: A review. *Renew. Sustain. Energy Rev.* **2010**, *14*, 112–129. [CrossRef]
43. Zhang, P.; Li, W.; Li, S.; Wang, Y.; Xiao, W. Reliability assessment of photovoltaic power systems: Review of current status and future perspectives. *Appl. Energy* **2013**, *104*, 822–833. [CrossRef]

44. Collins, E.; Dvorack, M.; Mahn, J.; Mundt, M.; Quintana, M. Reliability and availability analysis of a fielded photovoltaic system. In Proceedings of the 34th IEEE Photovoltaic Specialists Conference (PVSC), Philadelphia, PA, USA, 7–12 June 2009.
45. Billington, R.; Jonnavithula, A. Application of sequential Monte Carlo simulation to evaluation of distributions of composite system indices. *IEEE Proc. Gen. Transm. Distrib.* **1997**, *144*, 87–90. [[CrossRef](#)]
46. Billington, R.; Allan, R.N. *Reliability Evaluation of Power Systems*; Springer: Boston, MA, USA, 1984.
47. Quiles Cucarella, E.; Roldán Blay, C.; Roldán Porta, C.; Escrivá Escrivá, G. Accurate Sizing of Residential Stand-Alone Photovoltaic Systems Considering System Reliability. *Sustainability* **2020**, *12*, 1274. [[CrossRef](#)]
48. Roldan-Blay, C.; Roldan-Porta, C.; Peñalvo -López, E.; Escrivá-Escrivá, G. Optimal Energy Management of an Academic Building with Distributed Generation and Energy Storage Systems. *IOP Conf. Ser. Earth Environ. Sci.* **2017**, *78*, 012018. [[CrossRef](#)]
49. IDAE (Institute for Energy Diversification and Saving). *Energy Price Report: Fuels and Fuels*; IDEA: Madrid, Spain, 2022.
50. NREL (National Renewable Energy Laboratory). Champion Photovoltaic Module Efficiency Chart. Available online: <https://www.nrel.gov/pv/module-efficiency.html> (accessed on 23 May 2022).
51. Feldman, D.; Wu, K.; Margolis, R. *H1 2021 Solar Industry Update*; NREL: Golden, CO, USA, 2021.
52. Islam, S.N.; Saha, S.; Haque, M.E.; Mahmud, M.A. Comparative Analysis of Commonly used Batteries for Residential Solar PV Applications. In Proceedings of the 2019 IEEE PES Asia-Pacific Power and Energy Engineering Conference (APPEEC), Macao, China, 1–4 December 2019; pp. 1–5.
53. Sancho Ávila, J.M.; Riesco Martín, J.; Jiménez Alonso, C.; Sánchez de Cos Escuin, M.; Montero Cadalso, J.; López Bartolomé, M. *Atlas of Solar Radiation in Spain Using Data from the EUMETSAT Climate SAF*; AEMET: Madrid, Spain, 2012.

Disclaimer/Publisher’s Note: The statements, opinions and data contained in all publications are solely those of the individual author(s) and contributor(s) and not of MDPI and/or the editor(s). MDPI and/or the editor(s) disclaim responsibility for any injury to people or property resulting from any ideas, methods, instructions or products referred to in the content.